

Hydrogarnet: A Host Phase for Cr(VI) in Chromite Ore Processing Residue (COPR) and Other High pH Wastes

S. HILLIER,^{*,†} D. G. LUMSDON,[†]
R. BRYDSON,[‡] AND E. PATERSON[†]

Macaulay Institute, Craigiebuckler, Aberdeen AB15 8QH, UK,
and Leeds Electron Microscopy and Spectroscopy Centre,
Institute for Materials Research, SPEME, University of Leeds,
LS2 9JT, UK

For understanding both the environmental behavior and developing remediation treatments for chromium ore processing residue (COPR) it is important to identify all the potentially soluble sources of Cr(VI). Hydrogarnet has been identified as a major phase in COPR and it has been previously speculated that it has a capacity to host Cr(VI). Here we provide direct evidence of this capacity by demonstrating the incorporation of Cr(VI) into laboratory synthesized hydrogarnet. Electron microscopy and energy dispersive X-ray microanalysis show incorporation of approximately 17 000–22 000 mg Cr(VI) kg⁻¹ hydrogarnet. X-ray powder diffraction data show that peak intensities are altered by chromium substitution and that chromium substituted hydrogarnets have a smaller unit cell than the pure Ca–Al end member. This is consistent with substitution of hydroxyl tetrahedra by smaller chromate tetrahedra. Electron energy loss spectroscopy confirms the tetrahedral coordination and hexavalent oxidation state of chromium in the hydrogarnets. The maximum amount of hexavalent chromium that can be introduced synthetically corresponds to a replacement of about one out of every eight hydroxyl tetrahedral per unit cell by a CrO₄²⁻ tetrahedra and tallies closely with the amount of chromium measured in hydrogarnets from COPR. Chromium-bearing hydrogarnet is the most abundant crystalline phase in millions of tons of COPR contaminating land around Glasgow, Scotland, and was recently identified in COPR from sites in North America. Calculations based on its abundance and its Cr(VI) content indicate that hydrogarnet can host as much as 50% of the Cr(VI) found in some COPR samples.

Introduction

In previous work on the solid-state speciation of chromium in chromite ore processing residue (COPR) we have shown that chromium is associated with several crystalline mineral phases (1) known to have contrasting physicochemical properties. For Cr(VI), one of the minerals implicated was a hydrocalumite type phase, a calcium/aluminum layered double hydroxide, known to have anion exchange properties and subsequently shown to exchange chromate with sulfate

in laboratory experiments (2). Calculations based on quantitative mineralogical analysis of COPR and hydrocalumite compositions from sites in Scotland (1) indicate that around 4000 mg kg⁻¹ Cr(VI) is held in an exchangeable form in hydrocalumite. However, observations also suggested (1) that a similar amount of Cr(VI) was associated with hydrogarnet, a calcium aluminate common in many high pH wastes, which has no known anion exchange properties. It was speculated that Cr(VI) was structurally incorporated in hydrogarnet (1). The garnet structure consists of alternating tetrahedra and octahedra which share corners to form a three-dimensional network. In classic rock-forming garnets the tetrahedra are silica SiO₄⁴⁻ tetrahedra, whereas in hydrogarnet the tetrahedra are composed of four hydroxyls, H₄O₄⁴⁻. Octahedral sites in garnets are occupied by trivalent cations such as aluminum in 6-fold coordination. The cavities formed between the corner-sharing tetrahedra and octahedra have the shape of distorted cubes and contain divalent cations, such as calcium in 8-fold coordination. As an example, the end member hydrogarnet, known by its mineralogical name of katoite, has an ideal formula unit of Ca₃Al₂(H₄O₄)₃ and there are eight such formula units per unit cell (3). Hydrogarnet is a common phase observed in high-alumina cements (4) and in the cement literature this phase is written in a shorthand notation, C₃AH₆, denoting its oxide molar ratio, i.e., 3 mol of CaO, 1 mol of Al₂O₃, and 6 mol of H₂O.

In addition to its occurrence in cements, hydrogarnet occurs in a wide variety of other high pH environments and industrial waste streams. In COPR in Scotland it typically occurs as the main crystalline phase averaging around 25% by weight (1) and its presence has been recently confirmed (up to around 18 wt %) in COPR from New Jersey (5) in the United States. Hydrogarnet is also found in “muds” produced during the Bayer process (6), blast furnace slags (7), and lime-treated fly ashes (8), as well as in numerous situations where cement is used in the immobilization and containment of toxic wastes, including radioactive waste repositories (9). In all of these systems a variety of toxic metals and metalloids, including chromium, are present as oxyanions. As a result there have been numerous studies devoted to elucidating the mechanisms that affect the mobility of Cr(VI) in cement-based matrices (10–15). In this work we describe the laboratory synthesis of hydrogarnet in the presence of chromate and provide evidence for the incorporation of hexavalent chromium into the synthesized hydrogarnet phase. The results are clearly important because, although hydrogarnet is very stable in high pH environments and thus may immobilize Cr(VI), it dissolves readily as pH levels drop and then becomes a source of any Cr(VI) incorporated in its structure. This is of obvious importance in relation to efforts to model and understand the mobility of Cr(VI) in a wide variety of high pH systems where hydrogarnet is likely to form, as well as informing technologies designed to remediate land contaminated with COPR.

Materials and Methods

Synthesis of Hydrogarnet. Calcium aluminum hydrogarnets were synthesized using an appropriate stoichiometric mixture of CaO (Alfa Aesar 010923) and Al₂O₃ γ -alumina (BDH 100084D). The reagents were carefully weighed, ground, and mixed in an agate mortar and pestle, sealed in Teflon bombs with 20 mL of deionized water, and reacted at 150 °C in an oven for 6 days. Replicate experiments were performed in which chromate was added to the system as CaCrO₄ (Alfa Aesar 043333). For experiments made with CaCrO₄, the quantity of CaO was adjusted accordingly so as to maintain

* Corresponding author phone: +44 (0)1224 318611; fax: +44 (0)1224 311556; e-mail: s.hillier@macaulay.ac.uk.

[†] Macaulay Institute.

[‡] University of Leeds.

the Ca/Al molar ratio (3/2) appropriate for pure hydrogarnet. Three different chromate concentrations were tested: one corresponding to the stoichiometric proportion of chromate required to replace one in every 24 hydroxyl tetrahedra in the hydrogarnet unit cell, the second corresponding to a substitution of one in 12, and the third corresponding to a one in 3 replacement. The first of these concentrations was chosen because it corresponded approximately with the amount of chromium substitution observed in hydrogarnets found in the COPR studied by Hillier et al., (1), while the second and third concentrations were chosen so as to investigate the upper solubility limit of Cr(VI) in hydrogarnet. For brevity the chromium runs are hereafter referred to as 1/24, 1/12, and 1/3. Altogether, twelve runs were made, three without chromium, four each at the 1/24 and 1/12 concentrations, and one at the 1/3 concentration.

Scanning Electron Microscopy. Selected run products were carbon coated and examined by scanning electron microscopy (SEM) in a Philips XL20 instrument using secondary electron imaging and an accelerating voltage of 20 kV; qualitative elemental analysis was performed by energy dispersive X-ray (EDX) analysis using an Oxford Instruments Si(Li) energy dispersive spectrometer. Three of the samples synthesized in the presence of chromate were also examined as polished thin sections prepared by encapsulating the powder products in epoxy resin.

X-ray Powder Diffraction. X-ray powder diffraction (XRPD) data were collected on a Panalytical Expert Pro diffractometer, equipped with an X'celerator position-sensitive detector. All samples were mounted in 1 cm circular cavity holders, and spun at 30 rpm during data collection using Ni filtered Cu radiation. Scans were made between 5 and 75° 2 θ , using a 0.5° divergence slit and step size of 0.017°, counting for 100 s per step. Subsamples were spiked with National Bureau of Standards 640a silicon powder as an internal *d*-spacing standard. Phases were identified via comparison with patterns in the Powder Diffraction File, set 44, International Centre for Diffraction Data, 2001. Selected samples were ground in an agate mortar and pestle to further reduce particle size and mounted in thin-walled 0.5 mm diameter glass capillaries. The capillaries were spun at 300 rpm and examined in transmission geometry, using Cu K α 1 radiation selected by an incident beam hybrid monochromator; the instrument and detector were the same, however, the count time was increased to 500 s per step so as to increase precision. Peak height intensity was measured on background subtracted patterns using the peak search routine of the Bruker Eva Diffrac-Plus software. Unit cell parameters for hydrogarnet were refined with the Bruker AXS program Topas version 2.1, using the LeBail method and space group Ia3d.

Transmission Electron Microscopy. Transmission electron microscopy (TEM) was carried out using an FEI CM200 field emission gun instrument operated at 200 kV and fitted with an ultrathin window Oxford Instruments EDX detector and Gatan GIF200 electron energy loss spectroscopy (EELS) imaging filter. The specimens were prepared by dispersing and grinding the samples in methanol in an agate mortar and pestle and pipetting a few drops onto a copper TEM grid coated with a thin, holey amorphous carbon film. Thin sample areas overhanging holes in the support film were imaged and spectroscopically analyzed using EELS and EDX analysis. EEL spectra were recorded in selected area diffraction mode from single-crystal regions of approximately 170 nm in diameter using convergence and collection angles of <1 mrad and 6 mrad respectively. Both EDX and EELS spectra were quantitatively analyzed.

Results

Scanning Electron Microscopy. Examination by SEM showed that hydrogarnet was the main phase produced in both the

Ca–Al and in the Ca–Al–Cr based systems. Visually the Ca–Al -based products were white powders, whereas the Ca–Al–Cr-based products were all bright yellow. None of the runs examined were completely pure hydrogarnet, all contained various minor impurities which exhibited platy habits, indicative of layered structures. Hydrogarnets synthesized in the presence of chromate consistently crystallized in a dodecahedral form, whereas those synthesized in the absence of chromate crystallized in a combined dodecahedral-trapezohedral form (Figure 1). Some images of hydrogarnets with an octahedral form as found in COPR are shown in Figure 1 for comparison. Qualitative chemical analysis by EDX spectroscopy revealed that a small amount of chromium was always present in hydrogarnet crystals synthesized in the presence of chromium. Chemical mapping by EDX spectroscopy of polished sections of hydrogarnet crystals embedded in resin indicated that this incorporation of chromium was present throughout the projected area of the crystals (Figure 2). Qualitatively, the amount of chromium incorporated into the hydrogarnets appeared to be of similar level, irrespective of the original amount of chromium in the starting materials.

X-ray Powder Diffraction. XRPD confirmed that hydrogarnet was the main component in the products of all runs. Minor to trace amounts of portlandite (Ca(OH)₂) and boehmite (AlOOH) were found to be common impurities in many runs and, in runs containing chromium in excess of 1/24, an unnamed layered calcium chromate (PDF 42-0063), was commonly observed. This latter phase was also observed to be more abundant than hydrogarnet in the single run performed at a 1/3 concentration. Furthermore, the latter run, was also the only one in which unreacted calcium chromate was observed. In two of the chromium runs a peak at around 0.785 nm indicated the probable presence of a hydrocalumite-type phase, presumably a chromium-bearing hydrocalumite similar to that observed in COPR (1, 5). Comparison of the XRPD patterns of chromium- and non-chromium-bearing hydrogarnets indicated that the chromium-bearing examples had a significantly smaller unit cell size (Figure 3). Precise measurements indicated a cell edge length of 1.25760(3) nm for Ca–Al hydrogarnet, whereas cell edge lengths for those hydrogarnets synthesized in the presence of chromate were shorter by comparison, ranging between 1.25563(2) and 1.25594(4) nm (the number in parenthesis is the esd of the last digit). The relative X-ray peak intensities for the chromium and non-chromium bearing hydrogarnets were also notably different (See Supporting Information Table S1), particularly for the low angle peaks (e.g., (211), (220), (321), (400), and (420) peaks). Assuming preferential orientation effects can be ignored (XRPD peak intensity data were measured with capillary samples), this finding could be taken as evidence for a change in the X-ray structure factors, $F(hkl)$, due to substitution of Cr.

Transmission Electron Microscopy. An example of a Bright Field TEM image and the selected area diffraction pattern from the hydrogarnet crystal in the top right corner is shown in Figure 4. The diffraction pattern indexes to hydrogarnet crystal structure oriented along the [351] zone axis and exhibits a forbidden (103) reflection which could possibly be due to the inclusion of Cr in the unit cell. In the light of the XRPD data, specifically the observed increase in (211), the observation of intensity in the (103) spot could be explained by double diffraction in the electron diffraction pattern, i.e., two (211) type diffraction events, e.g., (211) + ($\bar{1}\bar{1}2$) = (103). All EDX spectra from the hydrogarnet-type phase were similar to the one shown in Figure 4; these exhibited an approximate metal composition, in terms of atom%, of Al 40–42%, Ca 55–57%, and Cr 2–3.5%.

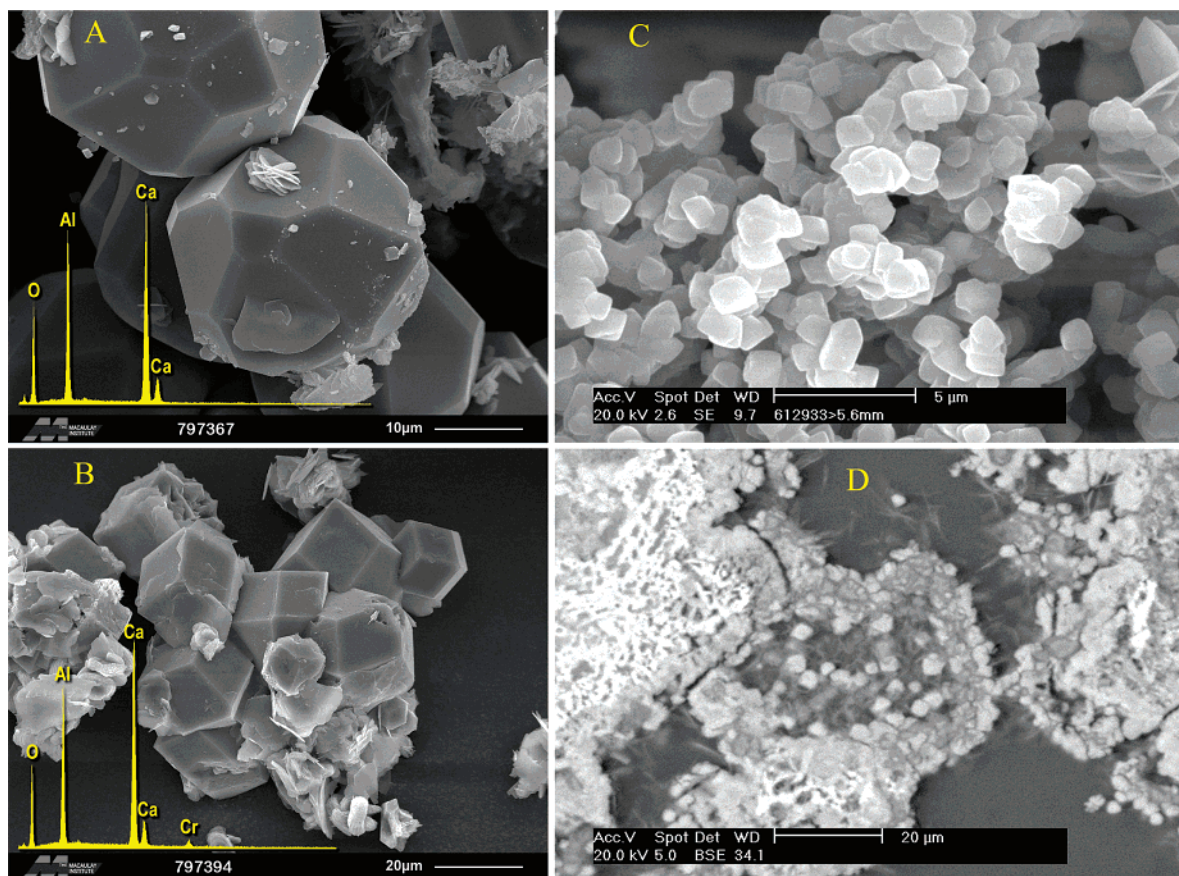


FIGURE 1. Examples of secondary electron SEM images and EDX spectra of synthesized hydrogarnets, without chromate (A) and with chromate (1/24) (B). Also shown for comparison are a secondary electron image (C) and a backscattered electron image (D) of hydrogarnets (most obvious in the center of the latter image) from COPR collected from Glasgow, Scotland.

Figure 5 shows the detail of the electron energy loss near edge structure (ELNES) Cr $L_{2,3}$ -edge spectral region both as recorded (inset in Figure 5) and following background subtraction. Note the data shown in Figure 5 are somewhat noisy due to both the low levels of Cr present, and the requirement of avoiding specimen damage (as observed at the O K-edge, see Supporting Information). As the Cr $L_{2,3}$ -edge is small and is superimposed on the background of the preceding oxygen K-edge, it is extremely difficult to subtract a reliable background beneath the Cr $L_{2,3}$ -edge. However, as the oxygen K-edge is only smoothly varying in this region and, for the purposes of the identification of the Cr valency and coordination, we are only really interested in the shape and the energy position of the Cr $L_{2,3}$ -edge, Figure 5 simply displays the result of an approximate background subtraction. The spectrum in Figure 5 reveals that the main Cr L_3 peak exhibits a maximum slightly above 580 eV together with a lower energy pre-peak or shoulder. The higher energy L_2 peak at around 590 eV has a similar, albeit broader, form. This distinctive Cr $L_{2,3}$ -ELNES has been observed previously (16, 17) and may be related to transitions from the chromium 2p level to the unoccupied e and t_2 molecular orbital structure of a transition metal in tetrahedral coordination. The energy position of the main Cr L_3 -peak maximum together with the shape and intensity ratio of the Cr L_3 - and Cr L_2 - white lines would both tend to indicate that Cr in hydrogarnet exists predominantly in the +VI oxidation state tetrahedrally coordinated to oxygen as the overall shape (notably the low energy shoulder) is very similar to that observed in the chromates $PbCrO_4$ and K_2CrO_4 (16, 17). In the latter works the energy position of the main Cr L_3 peak maximum in $PbCrO_4$ is quoted as being 580.9 eV (16), while the corresponding energy in K_2CrO_4 is quoted as being 581.6 eV (17);

note that both these spectra were recorded at energy resolutions different from that of the current work, one higher and one lower, respectively, which may slightly alter the position of the main peak maximum. Furthermore, the spectrum in Figure 5 is distinctly different from Cr in the III+ oxidation state in octahedral coordination to oxygen as is observed in spectra from say Cr_2O_3 (17, 18) where the Cr L_3 peak maximum is measured to be 579.0 eV and there is an absence of a clear low energy shoulder. Note that the splitting of the L_3 peak in the Cr $L_{2,3}$ -ELNES displayed in Figure 5 is perhaps slightly less than observed in the chromates $PbCrO_4$ and K_2CrO_4 (16, 17), which may perhaps suggest the presence of a longer Cr–O bond length in the case of the chromium-substituted hydrogarnet.

Discussion

Evidence for Chromate Substitution in Hydrogarnet. Hillier et al., (1) have suggested that a substantial proportion of the hexavalent Cr present in the COPR they studied was hosted in hydrogarnet. This inference was based on both stoichiometric considerations and indirectly on constraints from X-ray absorption near edge structure (XANES) studies of bulk COPR. Thus chromium was consistently identified as a component of hydrogarnet in COPR by microprobe analysis. Structural formulas calculated assuming that chromium was hexavalent and substituting in tetrahedral sites gave octahedral totals much closer to ideal (2 cations per formula unit) than if a trivalent oxidation state and octahedral substitution was assumed (1). XANES results indicated that approximately 30% of total chromium in the bulk COPR material was present as Cr(VI) (19). The agreement between the XANES results and data on the solid-state speciation of chromium, derived from quantitative mineralogical analysis,

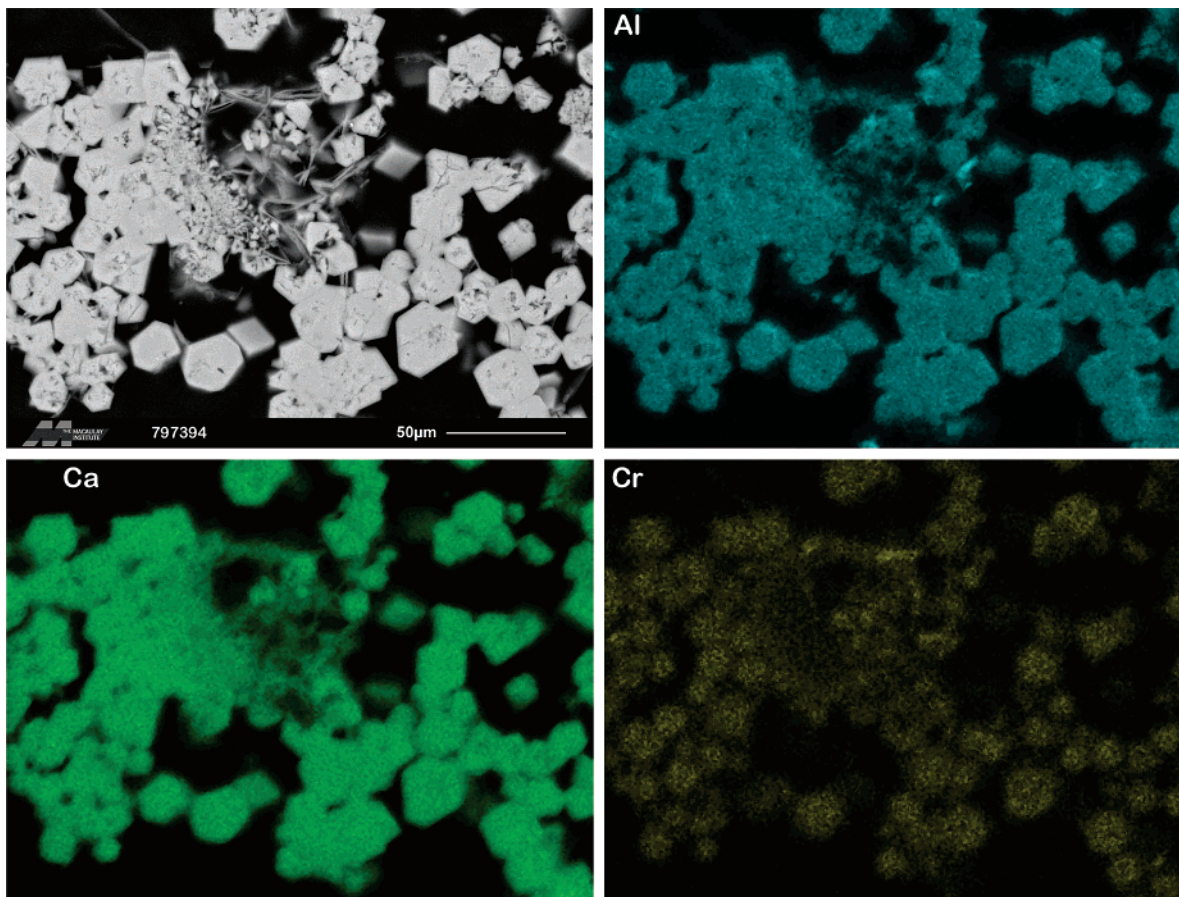


FIGURE 2. Backscattered electron image of polished thin section, and corresponding EDX maps showing the distribution of aluminum, calcium, and chromium in cross sections through numerous synthesized hydrogarnet particles.

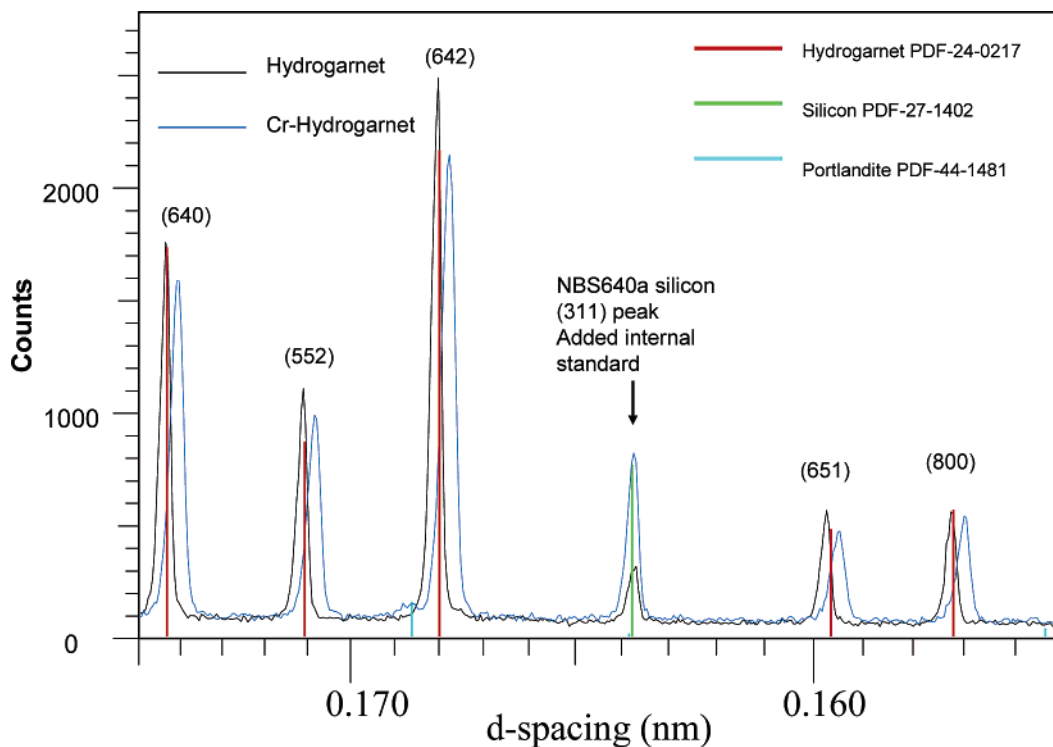


FIGURE 3. Portion of the XRPD patterns of two hydrogarnets, one synthesized with and one without Cr(VI), showing the obvious difference in *d*-spacings (and therefore unit cell size) with respect to the NBS640a silicon standard.

is improved if a hexavalent oxidation state for the chromium present in hydrogarnet is assumed (1). On both counts the evidence for the oxidation state of chromium in the hydro-

garnet in COPR is nonetheless indirect and Hillier et al., (1) duly noted this uncertainty. In terms of structural formulas the amount of chromium present in COPR hydrogarnets is

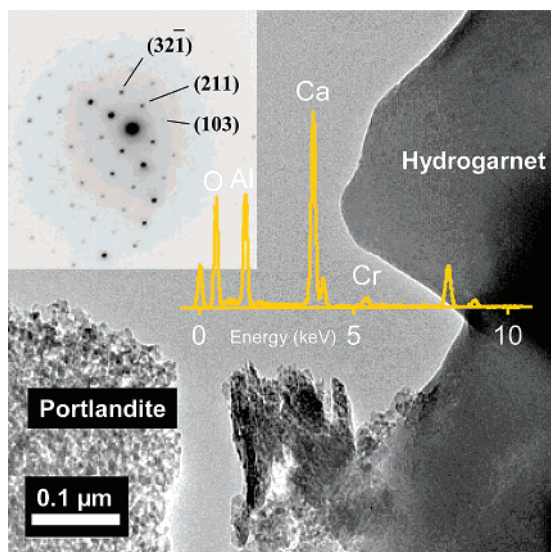


FIGURE 4. TEM Bright field image of hydrogarnet crystal and corresponding indexed diffraction pattern viewed down [351]. Insert is TEM-EDX spectrum of hydrogarnet. Metal Quantification (atom%) 42.3% Al, 55.4% Ca, 2.3% Cr, note Cu (and Zn) at ca. 8 keV are artifacts arising from stray scattering from the TEM sample holder and the TEM support grid.

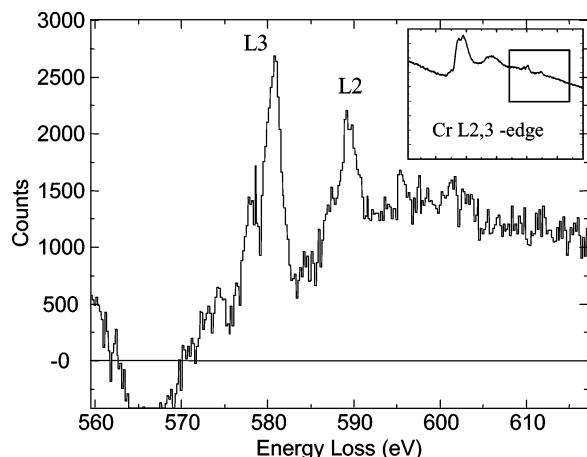


FIGURE 5. Cr $L_{2,3}$ -ELNES spectrum after approximate background subtraction before the edge on the decreasing signal of the oxygen K-edge; inset is the same EELS spectrum before background subtraction.

relatively small (a mean of 0.17 atoms per formula unit (1)), but because hydrogarnet is the most abundant phase in this COPR, ranging from about 20 to 30% by weight, it hosts in the order of 4000–6000 mg kg⁻¹ of chromium. This is approximately 10–15% of total chromium in this COPR. Thus if the chromium present in hydrogarnet is indeed Cr(VI), as postulated (1), then hydrogarnet is quantitatively as important a reservoir of hexavalent chromium in this material as the other major host of Cr(VI), i.e., hydrocalumite. In the case of hydrocalumite, however, Cr(VI) is held as an exchangeable anion whereas in hydrogarnet the chromium is incorporated in the structure. In the context of understanding processes controlling the release of Cr(VI) from COPR (20) and the potential for successful future remediation, the importance of confirming the oxidation state of chromium in substituted hydrogarnet is clear.

COPR is a complex mixture of at least ten crystalline phases together with a substantial X-ray amorphous component and with Cr(IV) present in several forms. The analysis of COPR to further investigate the oxidation state of chromium in

hydrogarnet is confounded by the complexity of this mixture. The alternative approach that we have adopted was to synthesize hydrogarnet in the presence of a source of Cr(VI) to determine if hexavalent chromium could be incorporated into the synthetic hydrogarnet structure.

The starting material for the hydrogarnet synthesis contained calcium chromate (chromatite) as the source of Cr(VI) and analyses of the run products by SEM showed that chromium is indeed incorporated into the synthetic hydrogarnets. Chemically, a change in the oxidation state of chromium over the duration of the experiment is unlikely since the conditions of synthesis favor maintaining Cr in the hexavalent form. The estimated pH of the mixture is in the region of 12, ensuring that CrO₄²⁻ was the predominant species. Furthermore the mixture did not contain any reducing agent so Cr(III) species would not have been produced. The redox transformation of Cr(VI) into Cr(III) can only take place in the presence of another redox couple (21) which provides the three electrons required to reduce CrO₄²⁻ into Cr(III). Qualitative SEM EDX results, including the elemental X-ray mapping of sections through the synthetic hydrogarnet crystals, clearly demonstrate that some chromium has been incorporated into the body of the hydrogarnets. From the known chemistry of the system it can be confidently presumed that this is incorporated as Cr(VI).

We are not aware of any previous reports of Cr(VI) substitution in hydrogarnet. Indeed, He and Suito (12) commented that chromium was absent in hydrogarnets formed by the hydration of tricalcium aluminate (C3A) in solutions containing an initial 50 ppm Cr(VI). These experiments (12) were conducted for a period of 30 h at 20 °C and the concentration of Cr(VI) in solution was observed to drop rapidly to less than 0.5 ppm within 6 h. Cr(VI) was incorporated into an abundant hydrocalumite phase that was present in the run products along with hydrogarnet. Hydrocalumite (AFm in cement notation) phases are often observed as the first hydration products of calcium aluminates and subsequently convert to hydrogarnet (4). Thus, in these experiments (12) the concentration of Cr(VI) may have been rapidly reduced by the initial formation of hydrocalumite, preventing its incorporation into hydrogarnet over the duration of the experiment, since hydrocalumite was still a major phase when the runs were terminated.

In contrast, hydrogarnets with trivalent chromium substituting in octahedral sites have been synthesized previously (10) including a strontium chromium hydrogarnet (22). Kindness et al. (10) reported a value of 1.2624 nm for the cell edge length of a Cr(III)-substituted hydrogarnet with an Al/Cr ratio of ~0.6. They noted that the unit cell was larger than that for pure calcium–aluminum hydrogarnet, taken as 1.25727 nm by reference to data in the Powder Diffraction File (PDF 24-217). Other examples of precisely measured unit cell parameters for pure hydrogarnet at ambient conditions indicate values around 1.257 nm, for example Lager et al. (23) give a value of 1.25731(2) nm. In the present investigation, we found that the size of the unit cell of hydrogarnet synthesized in the presence of chromate was significantly smaller than literature values for pure Ca–Al hydrogarnet (katoite). Direct comparison of XRPD patterns from pure and from Cr-bearing hydrogarnet, synthesized and analyzed under precisely the same experimental conditions, provides an unequivocal illustration of this result (Figure 3). The difference in the unit cell size between the absence and presence of chromium suggests that chromium has substituted into the hydrogarnet structure. Based on the SEM evidence alone, factors such as occlusion of another phase during precipitation and growth could not be excluded as the mechanism of chromium incorporation. In rock-forming garnets and in synthetic garnets it has been shown

that the hydrogarnet substitution ($\text{H}_4\text{O}_4^{4-} \leftrightarrow \text{SiO}_4^{4-}$) in terms of katoite and grossular end members causes the expansion of the tetrahedral site as the katoite component increases with a consequent increase in the unit cell size (24–26). In the end member, katoite, all tetrahedra are composed of four hydroxyls and all tetrahedral sites are vacant. The reduction in the size of the unit cell observed in the present study is therefore compatible with a substitution into the tetrahedral site, in a manner analogous to the substitution of silicon into this site in grossular-katoite solid solutions. Chromium substitution into the tetrahedral site effectively as a chromate anion is the obvious candidate. Indeed the bond lengths of Si–O and Cr–O would be expected to have similar values of around 0.16 nm (27, 28) and therefore similar effects on unit cell size. It is also worth noting that observations by Omotoso et al. (29) led them to speculate that small amounts of Cr(VI) may occupy tetrahedral sites, normally occupied by Si, in the X-ray amorphous C–S–H phase produced by hydration of tricalcium silicate. Others though have discounted any significant role for this phase in chromium uptake (10, 12).

Increasing the concentration of chromate in the laboratory experiments failed to result in a concomitant increase in chromium incorporated into the hydrogarnets. Instead the coprecipitation of other chromium-bearing phases was observed. This behavior indicates that the substitution of Cr(VI) into hydrogarnet is most likely limited by crystallochemical constraints. As pointed out previously (1), the tetrahedral structure of the chromate anion is likely to be a factor enabling it to substitute for hydroxyl tetrahedra. It would also lead to a local charge imbalance requiring compensation by either fewer hydroxyls or fewer cations in other sites, a factor likely to limit the extent of the substitution. The Ca/Al ratio of hydrogarnet single crystals measured by EDX in the TEM is within experimental error (approximately 5–10%) of the expected ratio (ideally 3/2) for hydrogarnet. If the measured chromium is alternatively assumed to substitute for aluminum in octahedral sites, a greater deviation from the expected ratio would result and should have been detected, which suggests that it does not. It is also notable that the extent of substitution observed in the laboratory synthesized hydrogarnets by TEM/EDX, at 2–3.5 atom percent chromium, corresponds very closely with that observed in the hydrogarnets formed in the field at COPR-contaminated sites (1).

Finally, the EELS data collected on individual hydrogarnet crystals provide direct spectroscopic evidence that the chromium incorporated into the hydrogarnets is tetrahedrally coordinated and in the hexavalent form. Taken together with the SEM and the XRPD data, the evidence for the ability of hydrogarnet to accommodate a limited amount of Cr(VI) in its structure is compelling.

Environmental Implications. The importance of understanding the interaction and incorporation of chromate in phases common in high-pH environments, such as hydrocalumite (AFm) and ettringite (AFt), has been widely recognized in the literature (10, 12, 15, 30–32). In a recent review evaluating the potential of ettringite and hydrocalumite in relation to the immobilization of heavy metals (14) hydrogarnet was discounted as a phase with a potential role in the immobilization of hazardous oxyanions. Our evidence for the incorporation of chromate in the hydrogarnet structure indicates that this view requires revision.

Our results show that about 1 atom of Cr(VI) per unit cell may be incorporated into synthesized hydrogarnet. On the basis of a structural formula expressed as $\text{Ca}_3\text{Al}_2(\text{H}_4\text{O}_4)_3$ (recall that there are eight such formula units in the unit cell) this equates to 0.125 atoms Cr(VI). On this same basis, Hillier et al. (1) recorded a mean value of 0.17 atoms of chromium in COPR hydrogarnet. These values equate to approximately

17 000–22 000 mg Cr(VI) kg^{-1} of hydrogarnet. The significance of this amount of Cr(VI) incorporation can be judged from characteristics of the COPR deposits around Glasgow, where it is estimated that 2.5×10^6 tons of COPR have been used as landfill (33), with typical hydrogarnet contents of more than 20% by weight (1). Furthermore, a recent quantitative mineralogical study of New Jersey COPR (5) records a clear deficit with respect to the total amount of Cr(VI) that can be accounted for if hydrocalumite type phases are considered as the only mineralogical hosts for Cr(VI). Hydrogarnet accounts for up to 18 wt % of these samples. We are not aware of any data on whether the hydrogarnet in these samples contains chromium, but it was noted (5) as one possible additional host for Cr(VI). Based on our results, we speculate that it is likely to be a host of some importance for a large part of the Cr(VI) that (in terms of which solid phase it is associated with) is otherwise unaccounted for (5).

In a wider context it is also tempting to speculate that other metal and metalloid oxyanions that are commonly tetrahedrally coordinated, for example As, Mo, and Se, may also be able to substitute to a limited extent into the hydrogarnet structure. This suggests a possible and hitherto overlooked role for hydrogarnet in relation to the mobility and availability of such elements in a wide variety of materials. Indeed, although layered double hydroxides such as hydrocalumite phases have been identified as important phases governing the behavior of hexavalent chromium in COPR (1, 2, 5) these phases are often transitory to hydrogarnet as a more stable phase (4). Our results imply that any factors that either promote or adversely affect hydrogarnet stability are likely also to affect the behavior of Cr (VI) in COPR.

Acknowledgments

This work was supported by the Scottish Executive Environmental and Rural Affairs Department. Evelyne Delbos is thanked for help with SEM and Carolyn Thomson is thanked for performing some of the syntheses. We acknowledge the use of the EPSRC's Chemical Database Service at Daresbury. The comments of four anonymous reviewers were most helpful.

Supporting Information Available

Table S1, measured X-ray powder diffraction intensities for chromium and non chromium bearing hydrogarnets and Figure S1 and text related to Electron Energy Loss Spectroscopy measurements. This material is available free of charge via the Internet at <http://pubs.acs.org>.

Literature Cited

- Hillier, S.; Roe, M. J.; Geelhoed, J. S.; Fraser, A. R.; Farmer, J. G.; Paterson, E. Role of quantitative mineralogical analysis in the investigation of sites contaminated by chromite ore processing residue. *Sci. Total Environ.* **2003**, *308*, 195–210.
- Geelhoed, J. S.; Meeussen, J. C. L.; Roe, M. J.; Hillier, S.; Thomas, R. P.; Farmer, J. G.; Paterson, E. Chromium Remediation or Release? Effect of iron(II) sulfate addition on chromium(VI) leaching from columns of chromite ore processing residue. *Environ. Sci. Technol.* **2003**, *37* (14), 3206–3213.
- Smrcok, L. Rietveld refinement of $3\text{CaO}\cdot\text{Al}_2\text{O}_3\cdot 6\text{H}_2\text{O}$. *J. Appl. Crystallogr.* **1987**, *20*, 320–322.
- Taylor, H. F. W. *Cement Chemistry*; Thomas Telford: London, 1997.
- Chrysochoou, M.; Dermatas, D. Application of the Rietveld method to assess chromium(VI) speciation in chromite ore processing residue. *J. Hazard. Mater.* **2006**; doi:10.1016/j.jhazmat.2006.05.081
- Whittington, B. I.; Cardile, C. M. The chemistry of tricalcium aluminate hexahydrate relating to the Bayer industry. *Int. J. Miner. Process.* **1996**, *48*, 21–38.
- Qian, G. I.; Sun, D. D.; Tay, J. H.; Lai, Z.; Xu, G. Autoclave properties of kirschsteinite-based steel slag. *Cem. Concr. Res.* **2002**, *32*, 1377–1382.

- (8) Duchesne, J.; Reardon, E. J. Lime treatment of fly ash: characterization of leachate composition and solid/water reactions. *Waste Manage.* **1999**, *19*, 221–231.
- (9) Ramirez, S.; Vieillard, P.; Bouchet, A.; Cassagnabere, A.; Meunier, A.; Jacquot, E. Alteration of the Callovo-Oxfordian clay from Meuse-Haute Marne underground laboratory (France) by alkaline solution. I. AXRD and CEC study. *Appl. Geochem.* **2005**, *20*, 89–99.
- (10) Kindness, A.; Macias, A.; Glasser, F. P. Immobilization of chromium in cement matrices. *Waste Manage.* **1994**, *14*, 3–11.
- (11) Rodriguez-Pinero, M.; Pereira, C. F.; De Elvira, C. R. Stabilization of a chromium-containing solid waste: immobilization of hexavalent chromium. *J. Air Waste Manage. Assoc.* **1998**, *48*, 1093–1099.
- (12) He, H.; Suito, H. Immobilization of hexavalent chromium in aqueous solution through the formation of $3\text{CaO} \cdot (\text{Al,Fe})_2\text{O}_3 \cdot \text{Ca}(\text{OH})_2 \cdot x\text{H}_2\text{O}$ phase, ettringite and C-S-H gel. *ISIJ Int.* **2002**, *42*, 139–145.
- (13) Ochs, M.; Lothenbach, B.; Giffaut, E.; Uptake of oxo-anions by cements through solid-solution formation: experimental evidence and modeling. *Radiochim. Acta* **2002**, *90*, 639–646.
- (14) Chrysochoou, M.; Dermatas, D. Evaluation of ettringite and hydrocalumite formation for heavy metal immobilization: Literature review and experimental study. *J. Hazard. Mater.* **2006**, *136*, 20–33.
- (15) Park, J. Y.; Kang, W. H.; Hwang, I. Hexavalent Chromium Uptake and Release in Cement Pastes. *Environ. Eng. Sci.* **2006**, *23*, 133–140.
- (16) Brydson, R.; Garvie, L. A. J.; Craven, A. J.; Sauer, H.; Hofer, F.; Cressey, G. L_{2,3} edges of tetrahedrally coordinated d⁰ Transition-Metal Oxyanions XO₄ⁿ⁻. *J. Phys.: Condens. Matter* **1993**, *5*, 9379–9392.
- (17) Kurata, H.; Ishizuka, K.; Kobayashi, T. Near edge structure in electron energy loss spectra of chromium trioxide intercalated into graphite and some chromium oxides. *Bull. Inst. Chem. Res. Kyoto University, Japan* **1988**, *66*, 572–579.
- (18) McBride, S.; Brydson, R.; Analytical TEM and Surface Spectroscopy of Ceramics: the microstructural evolution in titanium-doped chromia polycrystals as a function of sintering conditions. *J. Mater. Sci.* **2004**, *39*, 6723–6734.
- (19) Geelhoed, J. S.; Meeussen, J. C. L.; Hillier, S.; Lumsdon, D. G.; Thomas, R. P.; Farmer, J. G.; Paterson, E. Identification and geochemical modeling of processes controlling leaching of Cr(VI) and other major elements from chromite ore processing residue. *Geochim. Cosmochim. Acta.* **2002**, *66*, 3927–3942.
- (20) Farmer, J. G.; Paterson, E.; Bewley, R. J. F.; Geelhoed, J. S.; Hillier, S.; Meeussen, J. C. L.; Lumsdon, D. G.; Thomas, R. P.; Graham, M. C. The implications of integrated assessment and modelling studies for the future remediation of chromite ore processing residue disposal sites. *Sci. Total Environ.* **2006**, *360*, 90–97.
- (21) Richard, F. C.; Bourg, A. C. M. Aqueous geochemistry of chromium: A review. *Water Res.* **1991**, *25*, 807–816.
- (22) Li, G.; Feng, S.; Li, L.; Li, X.; Jin, W. Mild hydrothermal syntheses and thermal behaviors of hydrogarnets Sr₃M₂(OH)₁₂ (M = Cr, Fe, and Al). *Chem. Mater.* **1997**, *9*, 2894–2901.
- (23) Lager, G. A.; Downs, R. T.; Origlieri, M.; Garoutte, R. High-pressure single-crystal X-ray diffraction study of katoite hydrogarnet: Evidence for a phase transition from Ia3d - > I43d symmetry at 5 Gpa. *Am. Mineral.* **2002**, *87*, 642–647.
- (24) Sacerdoti, M.; Passaglia, E. The crystal structure of katoite and implications within the hydrogrossular group of minerals. *Bull. Mineral.* **1985**, *108*, 1–8.
- (25) Lager, G. A.; Armbruster, T.; Rotella, F. J.; Rossman, G. R. The OH substitution in garnets: X-ray and neutron-diffraction, infrared and geometric-modeling studies. *Am. Mineral.* **1989**, *74*, 840–851.
- (26) Jappy, T. G.; Glasser, F. P. Synthesis and stability of silica substituted hydrogarnet Ca₃Al₂Si_{3-x}O_{12-4x}(OH)_{4x}. *Adv. Cement Res.* **1992**, *4*, 1–8.
- (27) Fletcher, D. A.; McMeeking, R. F.; Parkin, D. The United Kingdom Chemical Database Service. *J. Chem. Inf. Comput. Sci.* **1996**, *36*, 746–749.
- (28) Inorganic Crystal Structure Database (ICSD). FIZ Karlsruhe. *ICSD-WWW Interface*; Hewat, A.; Institut Laue-Langevin, 6, rue Jules Horowitz, BP 156 –38042 Grenoble Cedex 9 – France; <http://icsd.ill.fr/icsd>.
- (29) Omotoso, O. E.; Ivey, D. G.; Mikula, R. Hexavalent chromium in tricalcium silicate. Part 1. Quantitative X-ray diffraction analysis of crystalline hydration products. *J. Mater. Sci.* **1998**, *33*, 507–513.
- (30) Palmer, C. D. Precipitates in a Cr(VI)-contaminated concrete. *Environ. Sci. Technol.* **2000**, *34*, 4185–4192.
- (31) Perkins, R. B.; Palmer, C. D. Solubility of Ca₆(Al(OH)₆)₂SO₄·26H₂O, the chromate analog of ettringite, 5–75 °C. *Appl. Geochem.* **2000**, *15*, 1203–1218.
- (32) Perkins, R. B.; Palmer, C. D. Solubility of chromate hydrocalumite (Ca₃Al₂O₆·CaCrO₄·12H₂O), 5–75 °C. *Cem. Concr. Res.* **2001**, *31*, 983–992.
- (33) Farmer, J. G.; Graham, M. C.; Thomas, R. P.; Licon-Manzur, C.; Paterson, E.; Campbell, C. D.; Geelhoed, J. S.; Lumsdon, D. G.; Meeussen, J. C. L.; Roe, M. J.; Conner, A.; Fallick, A. E.; Bewley, R. J. F. Assessment and modelling of the environmental chemistry and potential for remediation of chromium-contaminated land. *Environ. Geochem. Health* **1999**, *21*, 331–337.

Received for review September 14, 2006. Revised manuscript received December 20, 2006. Accepted January 8, 2007.

ES0621997